PINSA, **67, A,** No. 1, January 2001, pp. 131-143
© Printed in India

OPTICAL PROCESSES IN NANOCRYSTALLINE SEMICONDUCTOR MATERIALS

S CHAUDHURI AND A K PAL

Department of Materials Science, Indian Association for the Cultivation of Science, Calcutta-700032 (India)

(Received 06 March 2000; Accepted 15 September 2000)

Optical processes in nanocrystalline semiconductors with special reference to the absorption and photoluminescence phenomena are discussed. Recent developments in the areas of several II-VI semiconductors *e.g.* ZnS and ZnSe along with their alloy ZnS_xSe_{1-x} (x~0.05) in nanocrystalline form are specially focussed in this report.

Key Words: Nanocrystalline Films; Optical Process; II-VI Semiconductors; Absorption; Photoluminescence

Introduction

In recent years advances in the areas of synthesis and characterization of semiconductors indicated that more exciting opportunities are lying ahead if the structure be scaled down to nanometer level[1-5]. Below a critical grain size, the characteristic properties of a material changes and become quite different from the corresponding bulk solid. Depending on the material concerned, the size dependent properties of interest may be related to mechanical, optical, electrical, electronic and optoelectronic applications. Considerable research activities in these areas have recently been demonstrated for different nanostructured semiconducting materials. The nanoparticles may be obtained as colliods, free standing powders as well as thin films. Structural and optical properties of the nanocrystalline materials may be investigated by different techniques such as, X-ray diffraction, transmission electron microscopy, atomic force microscopy, photoluminescence, optical transmittance, Raman studies etc. Due to the three dimensional carrier confinement there may be interesting properties[4,6-8] involving singularities in the density of states and improved linear and nonlinear optical responses[9,10]. From technological point of view II-VI semiconductors in nanocrystalline thin film form are of current interest for the realization of frequency selective lasers and photodetectors[11,12] whose performances may be modulated drastically by the shapes and sizes of the nanocrystallites. In addition, semiconductor nanostructures may be used to fabricate memories and microprocessors resulting in computer revolution. Possibility of obtaining quantum wells and quantum wires have practically revolutionized the semiconductor device physics. In semiconductor nanocrystallites or zero dimensional quantum dots a considerable fraction of the atoms reside on the surfaces of the devices or quantum dots and they consist of as few as 10^3–10^6 atoms. The carrier confinement resulting from band structure modification produces interesting physical properties with potential application in optical devices. The dependence of the electronic states of the quantum dots on the surrounding medium are not clearly understood till now. The optical properties of the quantum dots show blue shift due to carrier confinement. The quantum confinement stabilizes the excitonic effect and photoluminescence due to excitonic recombination may be expected at a higher temperature.

The experimental observations published so far on nanocrystalline materials were mainly on the elemental or binary compound semiconductors. Wide gap II-VI semiconductors, specially zinc chalcogenides, were the subject of numerous studies[9-10,13-17] in the past due to their high potential for various device applications. It may be mentioned here that the preparation of high quality doped ZnS has an inherent problem due to self-compensation effect. Most of the previous works on ZnS were concentrated on understanding and solving the problem of effective doping. Growth of ZnS layers on foreign substrates like GaAs was also the subject of many investigations in the past due to its use as thin film electroluminescent devices for flat panel displays[9]. Chen *et al.*[18] studied the absorption and luminescence in ZnS nanocrystals prepared by chemical precipitation route. They attributed the observed broad absorption band below the

absorption edge to the surface states present in the film. *Scholz et al.*[19] prepared ZnS nanocrystalline powders by using a chemical route and observed that the optical extinction spectra could be explained adequately by Mie scattering theory[20]. There is a need for more meaningful studies on this important material in nanocrystalline form so that the electron transport and optical processes in the material could be understood more faithfully. In recent times, ZnSe and ZnS_xSe_{1-x} alloys have also been extensively studied[21-26] for the realization of blue-light emitting diodes (LED) and laser diodes (LDs). Effective control of the electrical properties through doping (especially p-type) and reduction of lattice mismatch with GaAs substrate were the key issues to be investigated critically before these materials could be fruitfully exploited in the device technology. ZnS_xSe_{1-x} layers with x ~ 0.05-0.08 on GaAs which are perfectly lattice matched to the substrate[21,26] are well suited for fabricating LEDs and optoelectronic device applications in the blue-green spectral region.

A considerable progress has taken place in the theoretical understanding of the optical processes in nanocrystalline semiconductors, in general. Studies on the coherent transient optical effects in semiconductor nanostructures irradiated by lasers is one of the most interesting areas in current years. Here, we review the optical processes in nanocrystalline semiconductors, in general, with emphasis on two binary II-VI semiconductors ZnS and ZnSe and their alloy ZnS_xSe_{1-x} (x~0.05).

Preparation of Nanostructured Material

For the deposition of nanostructured materials different workers have used different techniques. High pressure sputtering, colloidal suspension, insertion of nanoparticles in porous zeolites, inclusion in glass prepared by conventional melting process etc. are worth to mention. CdS nanocrystallites having average size of 2.2 nm and 4.4 nm were synthesized by Nanda *et al.*[27] by a high temperature synthetic route. Focussed ion beams were also adopted by the workers for attaining structures below one micron. In fact, ionic exposures are useful to generate close packed structures with certain dimensional variation (100-600 nm). Deep UV radiation may also be used as a structure resolving tool. Among different techniques mentioned above, high pressure sputtering[27] is most attractive for preparing nanostructured material in thin film form and this technique is discussed here in some detail.

It is known that during sputtering the substrate temperature increases due to the impact of the particles ejected from the target particularly when the deposition is carried out at a stretch for a time longer than several minutes. This results in the increase of grain size through the increase of the adatom mobilities culminating in the coalescence of the crystallites. So, in order to get nanocrystalline films, sputtering should be done intermittantly at regular intervals of time to allow the oncoming adatoms to release their thermal energy before a second deposition is made. An electronically controlled shutter may be logically connected to the output of a thermocouple for this purpose, so that, the deposition is automatically stopped by the shutter whenever an increase in substrate temperature is recorded. This sequential sputtering is very useful for obtaining nanocrystalline films with controlled grain sizes throughout the thickness. Banerjee *et al.*[28] and Mandal *et al.*[29] have reported studies on optical and electrical properties of ZnSe[28,29] and ZnS[30] in nanocrystalline thin film form by using this sequential sputtering technique where the crystallite size was comparable to or less than the bulk exciton Bohr radius. Properties of $ZnS_{0.05}Se_{0.95}$ films, prepared by the same technique, have been studied by Gangopadhyay *et al.*[31].

(i) ZnS Films

Mandal *et al.*[29] deposited ZnS films onto quartz and freshly cleaved NaCl substrates by d.c. magnetron sputtering of a ZnS target (99.999%) in argon plasma at system pressure of ~40 Pa. The films were deposited at different substrate temperatures (210-300 K) and the duration of deposition was varied. The substrates were placed on a heavy copper block which could be cooled by liquid nitrogen or heated electrically to attain the desired temperature during deposition. The temperature of the substrate could be monitored and controlled by a copper-constantan thermocouple using an on/off electronic temperature controller. Before starting the actual deposition, the target could be pre-sputtered with a shutter located in between the target and the substrate. This shutter was also used to control the deposition time. All the depositions were performed at 1.5 kV and 50 mA with the target (2.5 cm dia) to substrate distance of ~2.5 cm.

Three sets of nanocrystalline ZnS films with different thicknesses of the order of ~10 nm, 15 nm and 40 nm were deposited by Mandal *et al.*[29] with substrate temperature within 210-300 K, corresponding to deposition times of ~8, 15 and 30 minutes respectively. An increase in substrate temperature by 5 K could be observed if the films were sputter-deposited continuously for 5-7 minutes. This rise in temperature was found to be localised at the film surface and no evidence of increase in the temperature of the copper substrate holder was observed. This culminated in unavoidable agglomeration of the adatoms and the films thus deposited did not have the signature of the nanocrystallites. To overcome this, the films were deposited in sequence of one minute by allowing them to dissipate their thermal energy for the next minute or so before the next deposition was started. Size quantization could be retained by depositing the films in the above sequence. The extent of size quantization remains the same for films having different thicknesses when deposited at a particular set of substrate temperature and system pressure in the plasma chamber. The films deposited onto quartz substrates were used for electrical/optical studies while the films deposited onto NaCl substrates were used for TEM observation.

(ii) ZnSe Films

Banerjee *et al.*[28] deposited nanocrystalline ZnSe films by d.c. magnetron sputtering of a ZnSe pellet (99.999% purity) in argon plasma at system pressures of 20 and 30 Pa. The films were deposited at 1.5 KV and 100 mA with target to substrate distance ~2.5 cm. Glass (Corning) or quartz (fused silica) and NaCl crystals were used as the substrates for optical and microstructural studies respectively.

(iii) $ZnS_{0.5}Se_{0.95}$ Films

Films with pre-assigned thicknesses were deposited by Ganguly *et al.*[31] by using the sequential sputtering technique, discussed above. Three sets of films with different thicknesses were deposited with substrate temperatures (T_s) of 203, 233 and 263 K. For each of these T_s values, films were deposited for two different deposition times (20 and 25 minutes) and for each deposition time and substrate temperature, the pressure of the plasma chamber was varied between 15-30 Pa. The thicknesses of the films, thus produced varied within 10-40 nm. Films were simultaneously deposited on quartz (for optical transmittance measurement), microscope grid (for microscopy) and GaAs (for photoluminescence measurement).

Microstructure of Nanocrystalline Films

The ZnS nanocrystalline films exhibited (Fig. 1) a zinc blende crystal structure as depicted by transmission electron diffraction pattern. The diffraction pattern showed three broad rings which could be assigned to the (111), (220) and (311) planes. The ring for (111) planes was most intense and broad. The intensity of the ring for (220) planes was weaker than those for both the rings. The widths of the rings for films deposited at lower substrate temperature (*i.e.* films having lower crystallite size) were broader than that for films deposited at higher substrate temperature. Fig. 2 shows the variation of crystallite size (D) with deposition temperature (T_s) for ZnSe films deposited

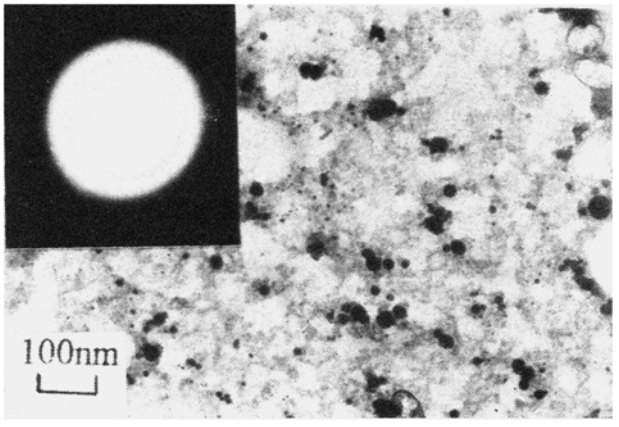

Fig. 1 TEM micrograph and corresponding diffraction pattern of a representative nanocrystalline ZnS film deposited at substrate temperature T_s = 233 K and pressure ~40 Pa

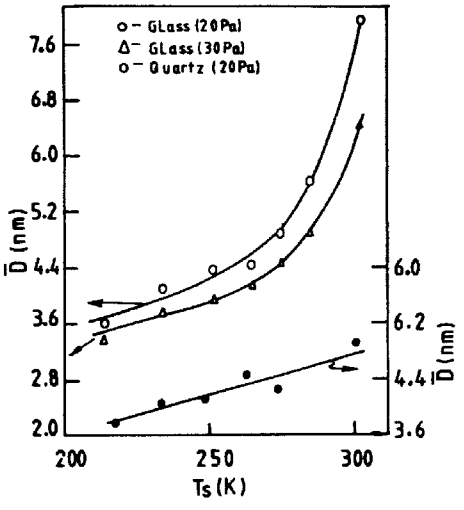

Fig. 2 Variation of crystallite size (D) with deposition temperature (T_s) for nanocrystalline ZnSe films deposited on glass and quartz substrates

on glass and quartz substrates. Fig. 3 (a & b) shows the TEM micrographs and the corresponding electron diffraction pattern of two representative $ZnS_{0.05}Se_{0.95}$ films deposited onto microscope grids at 233 K (15 Pa for 25 minutes) and 203 K (30 Pa and 20 minutes). One can observe that the films consisted of discrete nanocrystallites of dimensions varying between 1.7-2.1 nm and the diffraction patterns are mainly dominated by faint rings with a central halo. The films exhibited zinc blende structure and the rings could be identified as arising from (111), (220) and (311) planes.

Optical Absorption in Nanocrystalline Film

The absorption coefficients (α) of the nanocrystalline ZnS, ZnSe and $ZnS_{0.5}Se_{0.95}$ films were evaluated by measuring transmittance and reflectance[32] by a UV-VIS-NIR spectrophotometer (Hitachi U-3410). The band gaps (E_g) were determined by extrapolating $(\alpha h\nu)^2$ versus photon energy ($h\nu$) plots. The absorption trace for a representative film of nanocrystalline ZnS deposited at a substrate temperature of ~213 K with 30 minutes of deposition time is shown in Fig. 4. It may be noted that the variation of the absorption (α)

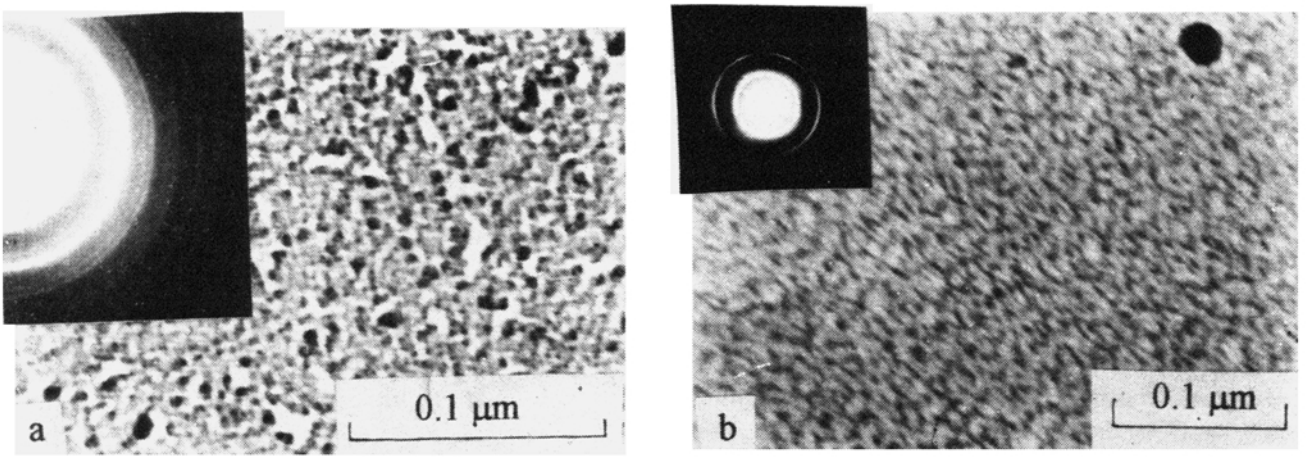

Fig. 3 TEM micrographs and corresponding diffraction patterns of two representative nanocrystalline $ZnS_{0.05}Se_{0.95}$ films deposited at (a) T_s=233 K (15 Pa for 25 minutes) and (b) T_s=203 K (30 Pa for 20 minutes)

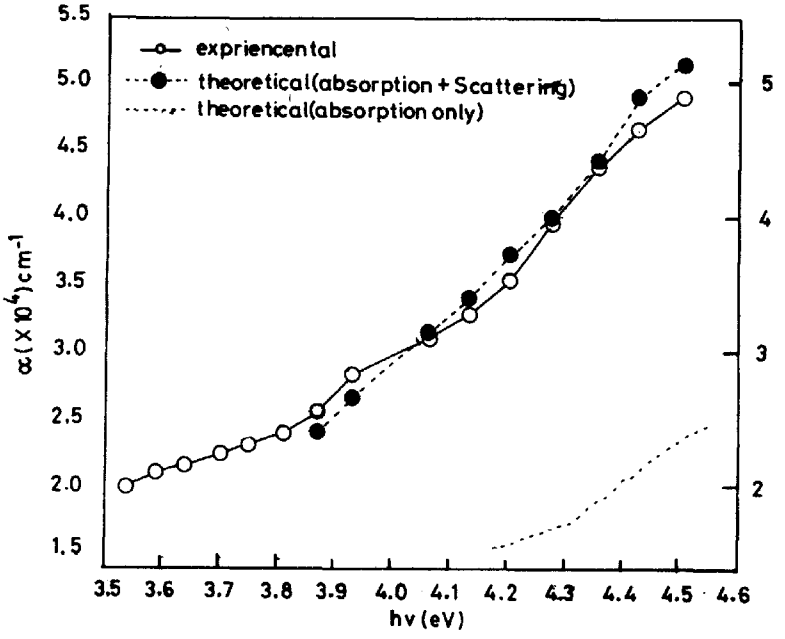

Fig. 4 Absorption trace of a representative nanocrystalline ZnS film deposited at a substrate temperature of ~213 K with 30 minutes of deposition

with the wavelength (λ) of the incident radiation were nearly the same for all the films. It was noticed that the fall of the absorption tail was sharper for films deposited for higher deposition time than those deposited for lower duration (*i.e.* for thinner films).

Fig. 5 shows the variation of band gaps of several nanocrystalline ZnS films deposited at different substrate temperatures and deposition times. The band gap values were always found to be higher compared to the bulk value. It may be noted that the films deposited at 213 K showed the maximum shift ($\Delta E_g = E_g - E_{g\,\text{Bulk}}$) of band gap from its bulk value (3.6 eV). The amount of shift in the band gap (ΔE_g) decreased substantially as the deposition temperature was increased. This is basically due to the fact that the films deposited at lower substrate temperature had smaller sizes of the nanocrystallite which was reflected in larger blue shift. Presence of smaller crystallite sizes would indicate the presence of an increasing amount of amorphous phase mixed with the nanocrystallites. This has been reflected in the gradual departure of the sharpness of the fall of the trace of transmittance (T_r) versus wavelength (λ) for films deposited at lower substrate temperatures. The average particle size, ($\bar{R}$), was measured from TEM studies and also from the curve fitting of the absorption data. It was observed that for a constant gas pressure in the chamber, the average particle size, ($\bar{R}$), increased (Fig. 6) with the increasing substrate temperature (T_S) upto ~300 K after which a sharp increase in the grain size was observed with increasing T_S. No agglomeration was observed till T_S ~300 K as the gas pressure probably did not cross the threshold limit for agglomeration. The crystallite size did not vary significantly as the deposition time was increased. The measurement of the band gaps of ZnS films deposited at higher temperature (> 320 K) indicated the films to be polycrystalline with band gap nearly equal to that of the bulk material.

Fig. 7 shows the room temperature optical absorption spectrum of a representative ZnSe film with band gap E_g=2.93 eV (for film deposited on glass). The shift of the fundamental band gap (due to the quamtum size effect) to the higher energy side in

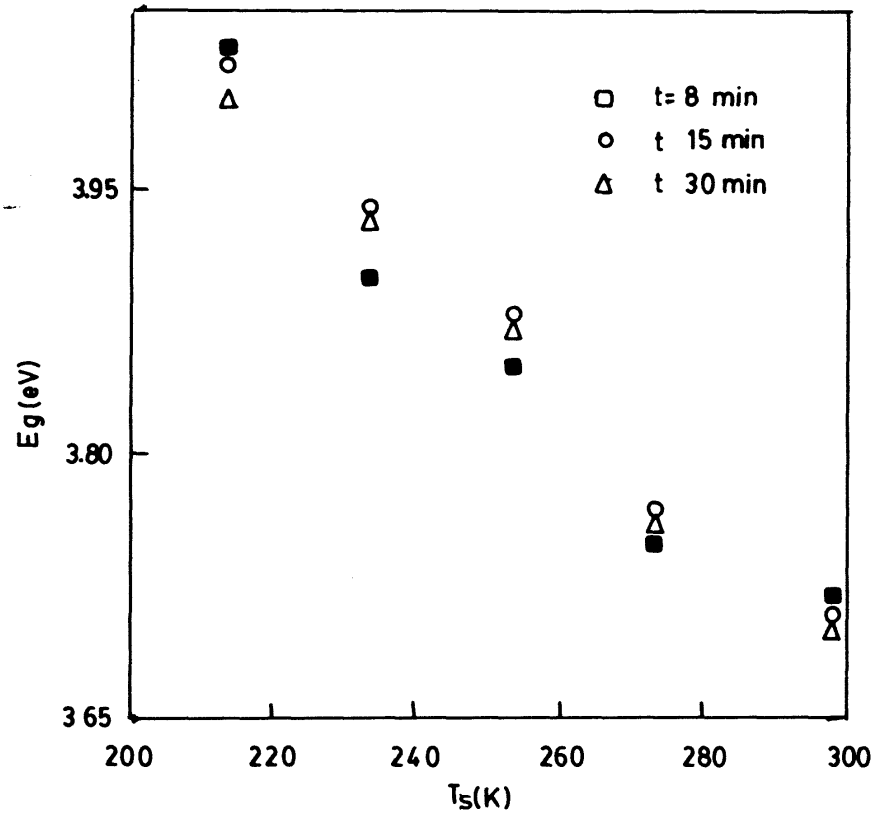

Fig. 5 Variation of band gap (E_g) of nanocrystalline ZnS films with substrate temperature (T_s) when deposited with various deposition times

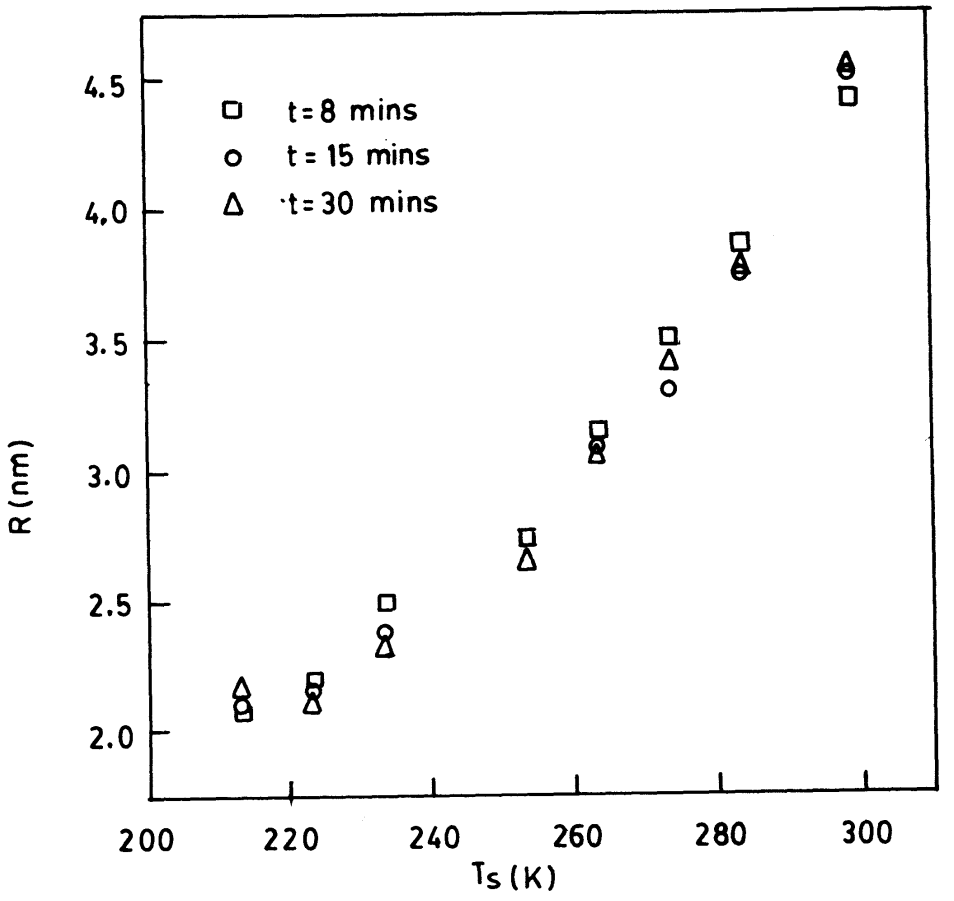

Fig. 6 (a) Variation of crystallite size (R) with substrate temperature (T_s) for nanocrystalline ZnS films deposited at various deposition times

comparison to the bulk value E_g^0=2.7 eV[33], may be noted. Table I shows the band gap (E_g) and crystalline radius (R) for different films deposited on glass substrate. As the films consisted of large number of nanocrystallites with different sizes and shapes, the absorption peak corresponding to level to level interband transitions was less sharp due to inhomogeneous broadening and room temperature phonon broadening effects[6,34,35]. Similar observations in other II-VI nanocrystallites have already been reported[4,6,34,36,37].

It may be noted that for $ZnS_{0.5}Se_{0.95}$ films the variation of the absorption coefficient (α) with energy ($h\nu$) of the incident radiation was nearly same for all the films. The fall of the absorption tail was sharper for films deposited for higher deposition time than those deposited for lower duration (*i.e.* for thinner films). The band gap (E_g) values of the nanocrystalline $ZnS_{0.05}Se_{0.95}$ films were always found to be higher (Table II) compared to the bulk value of 2.71eV obtained from the bulk values for ZnS and ZnSe

Table I

Values of band gap (E_g) grain size (R) estimated from the optical absorption studies of ZnSe films deposited on glass substrates at substrate temperature (T_s)) and pressure P. Values of grain size (R) from TEM studies (on NaCl substrate) are given

Film No.	T_s	P (Pa)	E_g (eV)	R (nm)	
				Optical	TEM
ZnSe-1	213	20	3.45	1.82	1.80
ZnSe-2	233	20	3.28	2.08	2.06
ZnSe-7	250	20	3.21	2.20	2.19
ZnSe-4	263	20	3.20	2.24	2.23
ZnSe-6	273	20	3.10	2.46	2.45
ZnSe-9	283	20	3.00	2.84	2.85
ZnSe-10	300	20	2.85	4.00	4.01
ZnSe-18	213	30	3.56	1.70	1.70
ZnSe-22	233	30	3.38	1.90	1.92
ZnSe-20	250	30	3.33	1.98	2.00
ZnSe-15	263	30	3.28	2.08	2.10
ZnSe-12	273	30	3.20	2.24	2.25
ZnSe-17	283	30	3.10	2.46	2.45
ZnSe-19	300	30	2.93	3.30	3.29

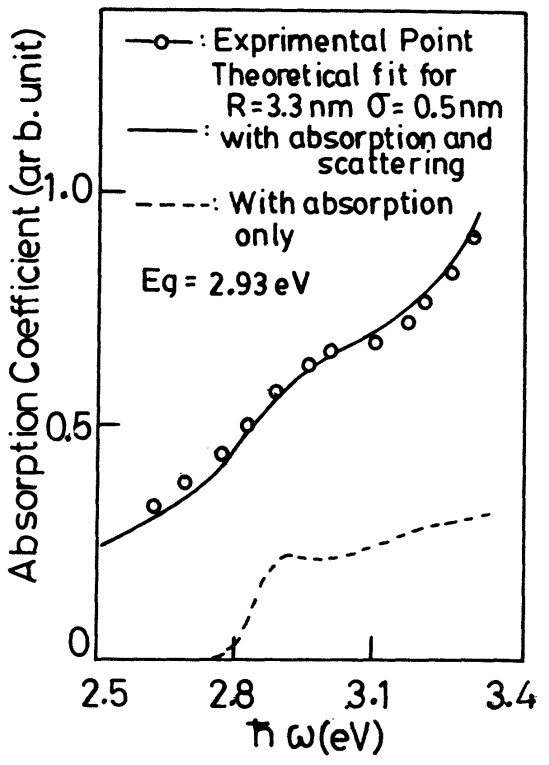

Fig. 7 Absorption spectra for a representative nanocrystalline ZnSe film deposited on glass at 300 K and 30 Pa

Table II

Values of average grain size (R) and band gap of nanocrystalline $ZnS_{0.05}Se_{0.95}$ films deposited at different conditions

Sample	Deposition Conditions	Band Gap E_g (eV)	Grain Size (nm)
ZSS-2	15 Pa 25 mins. 203 K	3.38	1.99
ZSS-1	15 Pa 25 mins. 233 K	3.46	1.88
ZSS-3	15 Pa 25 mins. 263 K	3.30	2.12
ZSS-4	20 Pa 20 mins. 203 K	3.36	2.02
ZSS-5	30 Pa 20 mins. 203 K	3.58	1.74
ZSS-7	15 Pa 20 mins. 203 K	3.32	2.09
ZSS-8	15 Pa 20 mins. 233 K	3.55	1.78
ZSS-9	15 Pa 20 mins. 263 K	3.40	1.96

using bowing relation given by Newbury *et al.*[25]. It may be noted that the films deposited at ~203 K and 30 Pa showed the maximum shift ($\Delta E_g = E_g - E_{g\,\mathrm{Bulk}}$) of band gap from its bulk value. The average particle size, ($\bar{R}$), was measured from TEM studies and also from the curve fitting of the absorption data. It was observed that the average particle size, ($\bar{R}$), did not show significant variation with the substrate temperature of deposition or gas pressure in the chamber. No agglomeration was observed till T_S ~300 K as the gas pressure probably did not cross the threshold limit for agglomeration. This observation is similar to that of nanocrystalline ZnS films. The crystallite size did not vary significantly as the deposition time was increased. It may be mentioned here that the bulk values of μ and E_g^o for $ZnS_{0.05}Se_{0.95}$ were computed from the value of the bowing parameter[4] along with the value of ε_o obtained from the linear extrapolation of the bulk values of ZnS and ZnSe.

The increase of the fundamental band gap of the nanostructred materials due to the quantum size effect (QSE) is well established. For the sake of comparison, we estimated the band gaps of these nanocrystalline films from

$$E_g = E_g^0 + \frac{\hbar^2\pi^2}{2\mu R^2} \; 1.786 \; \frac{e^2}{4\pi\varepsilon_o R} \; -0.248E_{RY}^* \qquad \ldots \quad (1)$$

for the strong confinement limit (*i.e* $R << a_B$) of QSE in nano material. For weak confinement limit (*i.e*, $R >> a_B$) we have:

$$E_g = E_g^0 + \frac{\hbar^2\pi^2}{2MR^2} - E_{RY}^* \qquad \ldots \quad (2)$$

where $M = m_e + m_h$, m_e and m_h being the electron and hole effective masses respectively. In equation (1), R is the radius of the nanocrystallites, $E^*_{RY} (= e^2/4\pi\varepsilon_o a_B)$ is the effective Rydberg energy for the bulk exciton with a_B as the corresponding Bohr radius ($= 4\pi\varepsilon_o \hbar^2/\mu e^2$), $\mu = [m_e m_h/(m_e + m_h)]$ being the reduced mass. E_g^o and ε_o are the band gap and low frequency dielectric constant respectively of the bulk material. By utilizing the average particle size, ($\bar{R}$), values as obtained from TEM measurements, the E_g values of different films were estimated from the above equation which were found to agree well with those obtained directly from the absorption spectra.

As the nanocrystalline films consist of large number of nanocrystallites with different sizes and

shapes, the absorption peak corresponding to level to level interband transitions will be less sharp (Fig. 2) due to the enhanced phonon broadening and inhomogeneity broadening effects[34,35]. The origin of the broadening due to inhomogeneity is generally ascribed to the fluctuation in the shape and size of the grains in the film. The deviation from the perfectly spherical shape of the particles would likely modify the selection rule and the transitions forbidden for the spherical form might appear in real situation. More over, the size distribution of the nanocrystallites would culminate in the fluctuation in the energy subbands as inferred from eqs. (1) and (2). Thus, the superposition of all the discrete absorptions due to these combined effects will result in broadening of the experimentally observed spectrum. It may be mentioned here that in this treatment, we have not taken into account the effect of the fluctuation in the shape of the crystallites on the absorption spectrum due to the inherent complexity of the problem.

The broadening due to phonon would also exist besides the above inhomogeneous broadening. This intrinsic broadening would have a finite value at room temperature. Klein *et al.*[38] considered this energy broadening due to phonon interaction in nanocrystalline systems and assuming the nanocrystallites to be spherical in shape having Gaussian size distribution, the total absorption was expressed as[34,37]:

$$\alpha = \int_{R_{min}}^{R_{max}} P(R)\ \alpha\ (R)\ dR \qquad \ldots (3)$$

where $P(R)$ is the probability of size distribution given by[34,39]:

$$P(R) = (R-R_{min})\ (R_{max}-R)\ \exp\ (-\frac{R^2}{\delta^2}) \qquad \ldots (4)$$

where R_{max} and R_{min} are the maximum and minimum diameters and δ is the half width of the distribution. $\alpha(R)$ is the absorption coefficient due to a nanocry stallite of radius R and can be written as[34,35]:

$$\alpha(R) = \frac{\omega}{n_0 c \varepsilon_0}\ (C_0/V)\ \frac{\hbar\Gamma}{(E_g-\hbar\omega)^2 + (\hbar\Gamma)^2} \qquad \ldots (5)$$

with,

$$C_0 = \frac{2\pi e^2\hbar^2}{m_e^2(\hbar\omega)^2}\ |p_{cv}|^2 \qquad \ldots (6)$$

where $\hbar\omega$ is the photon energy, n_0 is the refractive index, c is the velocity of light, V is the volume of the spherical nanocrystallite and p_{cv}, the bulk optical matrix element, is given by[4]:

$$|p_{cv}|^2 = (m_e/3)\ \frac{E_g\ (E_g+\Delta)}{(E_g+2\Delta/3)} \qquad \ldots (7)$$

Δ being the spin-orbit splitting factor.

Optical Loss Due to Scattering

It is apparent from Fig. 4 that the optical absorption solely cannot explain the shape and magnitude of the experimental absorbance spectra at room temperature. It is true that a large amount of incident light would be scattered by the ultra small crystallites. In this case, the total intensity (I_{SC}) of the scattered light per unit volume for normal incidence may be given by using the Mie scattering theory[20]. In the limit where the crystallite dimensions are much less than the optical wavelength (λ):

$$I_{sc} = \int P(R)\ I_{sc}(R)\ dR \qquad \ldots (8)$$

$$\text{with } I_{sc}(R) = (2/V)\ \left[(2\pi/\lambda)\ R^3\ \frac{(n_0^2-1)}{(n_0^2-2)}\right]^2 \qquad \ldots (9)$$

It may be noted that the authors did not consider the absorption due to surface traps and other impurities in these calculations as pointed out by Sekikawa *et al.*[40]. The theoretically simulated absorbance spectra for ZnS nanostructured films were obtained by using the eqs. (3) and (8) and are shown in Fig. 4. The amount of the optical loss due to scattering effect is easily estimated from the comparison between the theoretically simulated absorption curves. The values of different parameters utilized to compute the above simulated absorbance spectra for ZnS are as follows.

E_g=3.68 eV; m_e=0.27m_0; m_h=0.58m_0; ε_0=8.1; ε_∞=5.13; Δ=0.067; ω_{LO}=10.44 THz.

where, m_0 is the free electron mass. It can be observed that the simulated spectra fitted well with $\overline{R}$ value of 3 nm (with a mean fluctuation of ± 0.5 nm) for ZnS. This also agreed well with the nanocrystallite sizes determined from the transmission electron microscopy (TEM) and shift in the band gap[30].

Fig. 7 shows the absorption spectra of nanocrystalline ZnSe films. The values of different parameters[33] utilized to compute the theoretical absorption spectra for comparison with the experimental spectra of nano-ZnSe films are[33,41]:

E_g^0=2.7 eV; m_e=0.16 m_0; m_h=0.6 m_0; ε_0=9.14; ε_∞=6.3; Δ=0.403 and ω_{LO} =7.59 THz.

Similar studies on ZnTe and CdS in nanocrystalline were reported by Mandal *et al.*[42a]. Kulkarni *et al.*[42b] synthesized sulphide nanoparticles with particle diameter <5 nm using a chemical route.

Photoluminescence of Nanocrystalline Films

(i) ZnS

Photoluminescence (PL) spectra of the ZnS nanocrystalline films were recorded at 100 K with an exciting wavelength of 300 nm. The PL spectra of the films had a peak in the range of 350-400 nm. It can be seen (Fig. 8) that the line shapes of the PL spectra are asymmetric and broad. The film deposited at lower substrate temperature showed broader PL peak. Shift of these PL peaks to higher energies for films deposited at lower substrate temperature (*i.e.* with lower crystallite size) was visible for all the films irrespective of their thickness (*e.g.* deposition time).

The appearance of the PL peaks at energies substantially lower than the band gap suggests that transitions from energy states in the band gap are being favoured for the luminescence process in these nanocrystalline ZnS films. This observation

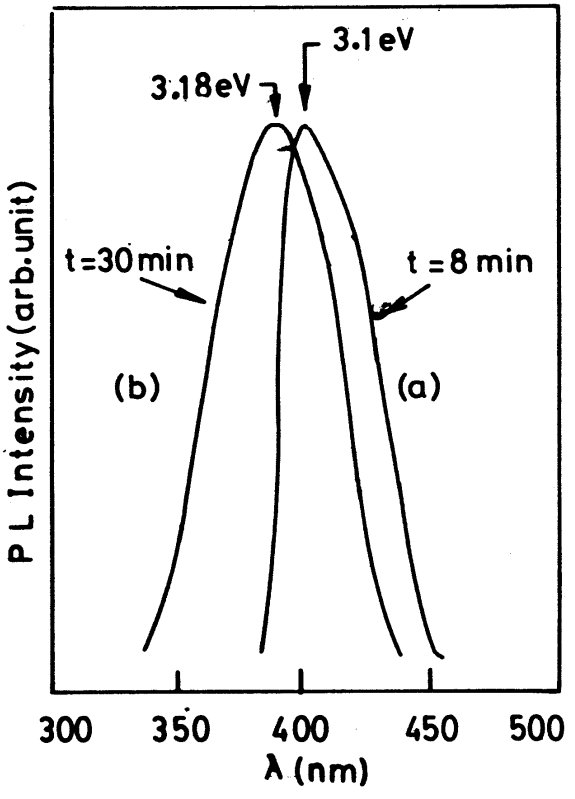

Fig. 8 PL spectra of two representative nanocrystalline ZnS films deposited at 233 K for (a) 8 minutes and (b) 30 minutes

may be ascribed to the presence of surface states of ZnS nanocrystallites constituting the film. This observation agrees well with that by Chen *et al.*[18]. The assignment of the surface states for the observed PL peak position at energies lower than band gap energy was also supported by the fluorescence and thermoluminescence measurements made by them. The density of surface states in nanocrystalline films would increase with the decrease in crystallite size constituting the film due to the increase in surface to volume ratio in films having smaller crystallites. This would reduce the probability of excitonic emission via nonradiative surface recombinations[18,40]. The band edge or excitonic emission will thus be effectively overlapped with the absorption of the surface states and as such would show photoluminescence at energies less than the band gap. The position of the PL peak would depend on the size of the nanocrystallite *i.e.* the substrate temperature during deposition. It was observed that the films deposited at lower temperature had lower crystallite size and the PL peak was shifted to higher energies. It is also interesting to note that thinner films deposited at a particular substrate temperature indicated peak position (Fig. 8a) at lower energies than that for a thicker film (Fig. 8b) deposited at the same substrate temperature. This is in commensurate with the fact that the surface to volume ratio will be higher for thinner films than that of thicker films. Thus the observed PL spectra supports the so-called trapped luminescence arising from the surface states. Similar crystallite size dependence of the shift of surface emission has also been reported by Chestnoy *et al.*[43].

(ii) ZnSe

The room temperature photoluminescence (PL) spectra for three representative ZnSe films deposited on quartz at 233, 273 and 300 K are shown in Fig. 9. The shift of the PL peak to higher energies for films deposited at lower T_S with lower grain sizes is quite clear from this figure. Similar changes in the peak position of PL spectra of other nanocrystalline semiconductors have already been reported by several groups[44-47]. Considering the fact that the PL spectrum is due to the radiative recombination of the lowest lying excited states of the nanocrystallites, the semi-quantitative estimation of the dependence of PL peak position on the average grain radius $\bar{R}$ may be obtained from the frame-work of effective mass relation as given by eq. (1) for grains with $R < a_B$ (a_B being the Bohr radius).

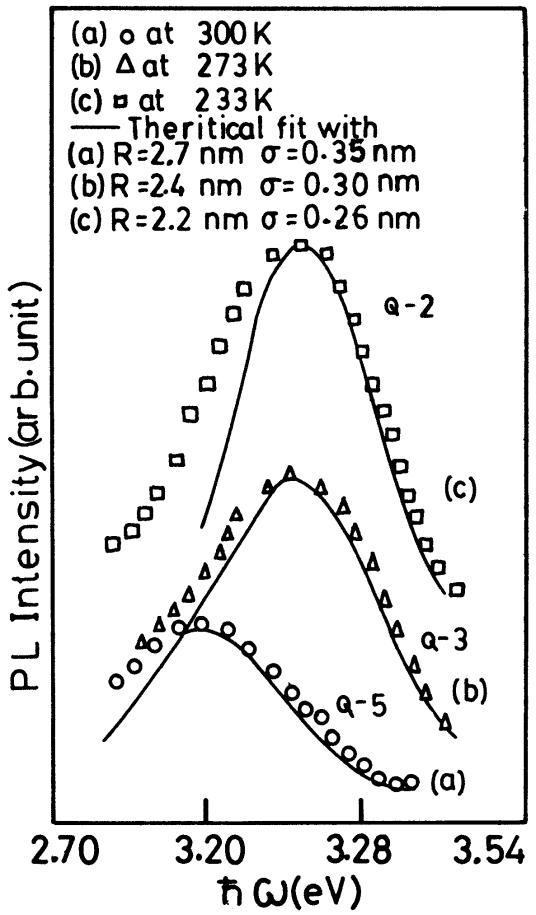

Fig. 9 Photoluminescence spectra of three representative nanocrystalline ZnSe films deposited on quartz substrate at 20 Pa and at different substrate temperatures as indicated in the figure

In general, the carrier confinement effect in semiconductor nanocrystallites stabilizes both excitons and corresponding luminescence due to excitonic recombinations even at room temperature. Systematic studies by different groups[48-50] indicated the presence of characteristic luminesence due to excitonic recombination in association with the significant contributions from impurities and surface states at the lower energy side of the PL spectrum. With the gradual decrease of the sizes of the nanocrystallites, the luminescence has been found to be dominated by band impurity and surface state transitions over the excitonic luminescence. However, the relative intensities depend on the excitation intensity. Ekimov *et al.*[44] have shown that with higher excitation intensity (so that the inter impurity luminescence becomes saturated) the transitions associated with the band to band free electron and hole would dominate in the PL spectra even for samples with smaller (~5.7 nm) grain size. Although the intensity dependence of PL studies were not done (due to the limitation of our present experimental set-up), it is believed that in the ZnSe specimen the highly intense PL peak is mainly due to excitonic recombination. This is guided by the fact that in the reverse situation (*i.e.* if it is due to impurity and surface states, for the sake of argument), the excitonic emission would arise at still higher energy side of the PL spectra. Consequently, the theoretically estimated grain size would be smaller than that obtained from the TEM and optical absorption studies. Similar treatment have been done earlier by Kohno *et al.*[47] for Si nanocrystallites.

Besides the peak position, the line shape of the PL spectrum is essentially given by the inhomogeneous broadening which is due to the size distribution of grains. The theoretical line shape $I(\hbar\omega)$ of the PL spectrum between the lowest energy state of the electron and hole ($1s_e \rightarrow 1s_h$) in a quantum dot with radius R may be expressed as[47]:

$$I(\hbar\omega) \propto \int g(R)|f(R)|^2\, \delta[\hbar\omega - E_L(R)]\, P(R)\, dR \quad \ldots (10)$$

where $g(R)$ is the carrier recombination probability, $P(R)$ is the grain radius distribution function, $f(R)$ is the oscillator strength and $E_L(R)$ is the emission energy which is given by eq. (1). Within the frame work of the effective mass approximation[46], the parameter $|f(R)|^2$ is proportional to R^{-9}. Following Kohno *et al.*[47], the explicit form of carrier recombination probability $g(R)$ is given by

$$g(R) = 1 \quad \ldots (11)$$

for $R > \bar{R}$, while for $R < \bar{R}$ we have :

$$g(R) = 2/\left[1 + (R/\bar{R})^2 \exp\{q\,(\frac{1}{R^2} - \frac{1}{\bar{R}^2})\}\right] \quad \ldots (12)$$

where

$$q = E_d/3\hbar\rho\, V_s \quad \ldots (13)$$

Here E_d is the deformation potential due to electron phonon interaction, ρ is the mass density and V_S is the velocity of sound in the material. Using eqs. (1), (10), (11), and (12), together with the parameters[33] E_d = 8.6 eV, ρ = 5.28 g cm^{-3} and V_S = 4.4 km sec^{-1}, the theoretical fits of the line shape of PL spectra corresponding to the ZnSe films deposited at 233 K, 273 K and 300 K on quartz substrates are shown in Fig. 9. The estimated average crystallite size, obtained from this best fit to the PL line shape, also agreed well

with that obtained from the absorption spectra and TEM studies.

From Fig. 9 it also appeared that the PL line shape becomes asymmetric for films having relatively, smaller grain sizes. Andrianasolo *et al.*[48] reported similar observation and by deconvolution of such asymmetrical PL spectrum they suggested the presence of additional peak at lower energy side due to carrier recombination between surface states. Moreover, in all cases we have noticed a small Stoke's shift between the peaks due to absorption and PL effects. Such shift is prominent for films having relatively smaller grain sizes, as is evident from Fig. 10. It is speculated that this might be due to the enhanced carrier recombination from relatively larger amount of surface states in smaller nanocrystallites. Similar observation have also been noticed by other workers in different nanocrystalline systems[47-50].

The existence of surface states in the fundamental band gap region is in fact not surprising for films having small grain size. Hache *et al.*[50] also pointed out the possibility of pair-state formation of the surface states, one near the valence band and the other near the conduction band. With the decrease of grain size, the ratio of the surface states to the volume states (*i.e.* size quantised states) would increase. This is due to the fact that many more atoms will reside at the surface of the grain rather than at a volume site. It is important to note that these surface states are intrinsic states and delocalized over the entire surface of the sphere. In this way they participate in the optical processes similar to the volume states[50].

(iii) $ZnS_{0.05}Se_{0.95}$

Photoluninescence (PL) spectra of the nanocrystalline $ZnS_{0.05}Se_{0.95}$ films deposited on GaAs (100) were recorded (Fig. 11) at 300 K with an exciting wavelength of 300 nm. The PL spectra of the films are dominated by a peak in the range of 360-370 nm with a distinct shoulder around 397 nm. It can be seen that the line shapes of the PL spectra are asymmetric and broad. Shift of these PL peaks to higher energies for films having lower crystallite size was visible for all the films irrespective of their thicknesses (*i.e.* deposition time).

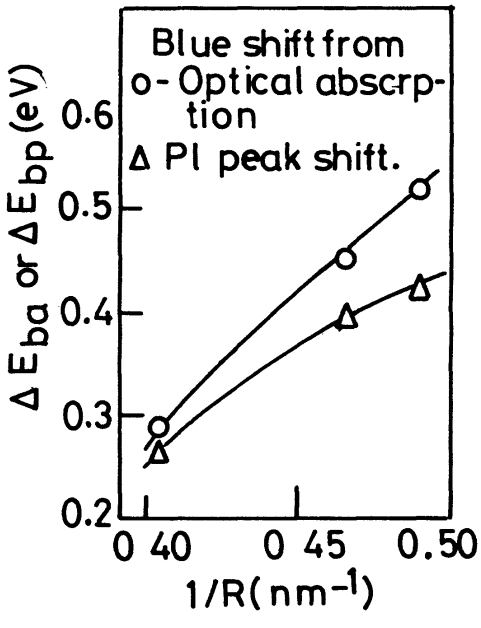

Fig. 10 Dependence of the blue shifts (ΔE_{bp} and ΔE_{ba}) of nanocrystalline ZnSe films, obtained from the optical absorption (ΔE_{ba}) and PL peak shift (ΔE_{bp}), on the 1/R, R being the average radius of the crystallites

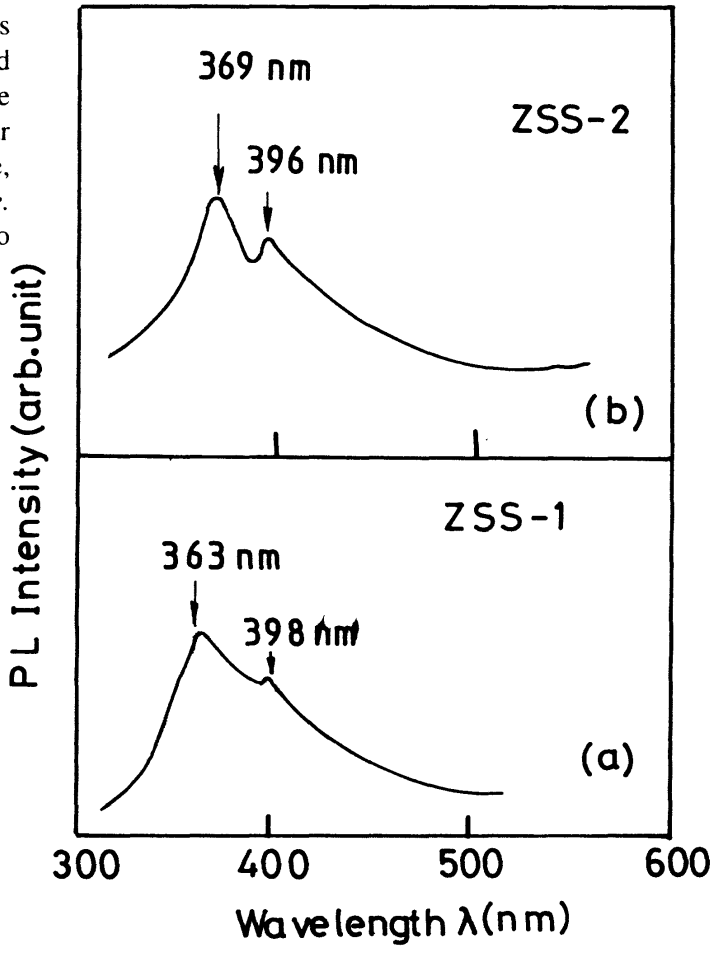

Fig. 11 PL spectra for two representative nanocrystalline $ZnS_{0.05}Se_{0.95}$ films deposited at 15 Pa for 25 minutes with substrate temperature : (a) 233 K and (b) 203 K

It could be observed that the sharp excitonic structure observed in the case of binaries (ZnS and ZnSe bulk) is replaced by a single, broad PL spectra for these nanocrystalline $ZnS_{0.05}Se_{0.95}$ films. This broadening may arise mainly due to alloy broadening and defect broadening. Alloy broadening may arise due to random distribution of sulphur atoms on selenium sites in these nanocrystalline films and as such an excited particle moving about the lattice would sense a varying local composition. As the lattice mismatch is small for films deposited onto GaAs, the broadening effect due to defects arising out of lattice mismatch may be minimal. But the surface states arising out of the enhanced ratio of surface atoms to the atoms constituting the main bulk of the $ZnS_{0.05}Se_{0.95}$ films would be very significant to cause defect related broadening. Similar observation for exciton line broadening in $ZnS_{0.05}Se_{0.95}$ epilayers grown on GaAs was reported by Newbury *et al.*[25]. The appearance of the shoulder at ~397 nm suggests the presence of transitions due to donor-acceptor (DA) pair formation. The origin of the DA transition may arise from Zn interstitials and/or sulphur vacancies causing donor levels and Zn vacancies causing acceptor states.

Conclusion

Nanocrystalline films of ZnS, ZnSe and $ZnS_{0.5}Se_{0.95}$ were deposited by high pressure magnetron sputtering technique. Films with different crystallite sizes were obtained by varying the substrate temperature during deposition and the thickness of the films could also be varied without sacrificing the blue shift. The films exhibited predominant zinc blende structure with intense rings for (111), (220) and (311) planes. The absorption behaviour in nanocrystalline films could not be explained from level to level transitions due to size quantization only. Significant contributions from inhomogeneity and phonon broadening effects along with optical losses due to scattering are required to be considered to explain the observed absorption behaviour. The PL spectra for nanocrystalline films indicated a presence of a broad absorption band at energy less than band gap energy. This suggested that transitions from energy states in the band gap are being favoured for luminescence process which could be attributed to the surface states present in these films. The thinner films indicated PL peaks at lower energies than those of thicker films in agreement with the higher surface to volume ratio for thinner films.

The PL spectra for nanocrystalline $ZnS_{0.05}Se_{0.95}$ films indicated the presence of a broad excitonic peak around 365 nm with a distinct shoulder around 397 nm. This broadening was attributed to the combined effects of alloy broadening and defect broadening due to enhanced surface states. The origin of the shoulder may be ascribed to DA transitions.

In reality, the exact nature of emission mechanism in semiconductor nanocrystallites is very much complex and a clear picture has not yet been emerged. Works done[51,52] in this area indicated that a significant role is played by the complicated strain distribution in the vicinity of the nanocrystallites and several fundamental mechanisms of carrier relaxation like multiphonon and Auger-like processes should be considered. Thus, the theoretical fit to the experimentally observed luminescence spectrum demands careful inclusion of all these effects.

Acknowledgements

Authors like to acknowledge with thanks the financial support from CSIR, Government of India and DST, Govt. of India during the tenure of the work on zinc chalcogenides carried out at IACS, Calcutta.

References

1 J Gutowski, N Presser and G Kudlek *Phy Stat Solidi (a)* **120** (1990) 11

2 H Hingerl, A Pesek, H Sitter, A Krost, D R T Zahn, W Richter, G Kudlek and J Gutowski 1990 *Proc SPIE : Physical Concepts of Materials for Optoelectronic Device Applications* **1361** (1990)

3 J M Hays, W Shan, X H Yang, J J Song and E Cantwell *Semicond Sci Technol* (1992) 1470

4 A D Yoffe *Adv Phys* **42** (1993) 173

5. W Gleiter *Nanostructured Mater* **1** (1992) 1

6 U Woggon and SV Goponenko *Phys Stat Solidi (b)* 189 (1995) 285

7 L Banyai and S W Koch *Semiconductor Quantum Dots, Series on Atomic, Molecular and Optical Physics* (World Scientific Publishing Co Singapore) **2** (1993)

8 L J Geerligs, C J Harmans and L P Kouwenhoven (Eds.) *The Physics of Few-electron Nanostructures, Physica (Utrecht)* **189 B,** (1993)

9 O N Djazovski, S Tanaka, H Kobayashi, N N Semienov and V V Pasynkov *Jpn J Appl Phys* **34** (1995) 4819

10 Y Chubachi *Thin Solid Films* **224** (1993) 184

11 W T Tsang *Semiconductors and Semimetals* (Eds: R K Willardson and A C Beer) Academic Press New York **24,** (1987) 397

12 S Schmitt-Rink, D S Chemla and D A B Milier *Advances in Physics* **38** (1989) 89

13 H Kinto, M Yagi, K Tazunori, T Yamada, H Uchiki and S Iida *J Cryst Growth* **117** (1992) 348

14 M Nagano, H Kanie, I Yoshida, M Sano and M Aoki *Jap J Appl Phys* **30** (1991) 1915

15 S Iida, T Yatabe, H Kinto and M Shinohara *J Cryst Growth* **101** (1990) 141

16 R Mach and G O Muller *J Cryst Growth* **86** (1988) 866

17 R H Mauch, R Menner and H W Schock *J Cryst Growth* **86** (1998) 885

18 W Chen, Z Wang, Z Lin and L Lin *J Appl Phys* **82** (1997) 3111

19 S M Scholz, R Vacassy, J Dutta and H Hoffmann *J Appl Phys* **83** (1998) 7860

20 M Born and E Wolf *Principles of Optics* (Pergamon Press) (1959) 664

21 C Thiandoume, O Ka, A Lusson, C Cohen, A Bouanani, M Rommeluere, A Tromson-Carli and O Gorochov *J Cryst Growth* **184/185** (1998) 149

22 I Suemune, K Yamada, H Masato, Y Kan and M Yamanishi *Appl Phys Lett* **54** (1989) 981

23 K Nakanishi, I Suemune, H Masato, Y Kuroda and M Yamanishi *Jpn J Appl Phys* **29** (1990) L2420

24 X H Yang, J M Hays, W Shan, J J Song and E Cantwell *Appl Phys Lett* **62** (1993) 1071

25 PR Newbury, K Shahzad, J Petruzello and D A Cammack *J Appl Phys* **66** (1989) 4950

26 H Hong, W A Anderson, J Haetty, A Petrou, E H Lee, H C Chang, M H Na, H Luo, J Peck and T J Mountziaris *J Appl Phys* **82** (1997) 4994

27 J Nanda, B A Kuruvilla, K V P M Shafi and D D Sarma *Physics of Semiconductor Nanostructures* (Ed. K.P Jain Narosa) New Delhi (1997) 25

28 S Banerjee, R Pal, A B Maity, S Chaudhuri and A K Pal *Nanostructured Materials* **8** (1997) 301

29 S K Mandal, S Chaudhuri and A K Pal *Nanostru Mater* **10** (1998) 607

30 S K Mandal, S Chaudhuri and A K Pal *Thin Solid Films* **350** (1999) 209

31. A Ganguly, S K Mandal, S Chaudhuri and A K Pal (comm)

32. D Bhattacharyya, S Chaudhuri and A K Pal *Vacuum* **43** (1992) 313

33 *Landolt Bornstein Numerical Data and Functional Relationships in Science and Technology* (Eds. O Madelung and M Schulz) New Series Group III Springer Verlag **22a,** 117

34 R Pal, D Bhattacharyya, A B Maity, S Chaudhuri and A K Pal *Nanostru Mater* **4** (1994) 329

35 S Schmitt-Rink, D A B Miller and D S Chemla *Phys Rev B* **35** (1987) 8113

36 L Brus *Appl Phys A,* **53** (1991) 465

37 J Allegre, G Arnaud, H Mathieu, P Lefebvre, W Granier and L Boudes *J Cryst Growth* **138** (1994) 998

38 M C Klein, F Hache, D Ricard and C Flytzanis, *Phys Rev B* **42** (1990) 11123

39 D Bhattacharyya, S K Bhattacharyya, S Chaudhuri and A K Pal *Vacuum* **43** (1992) 1201

40 T Sekikawa, H Yao, T Hayashi and T Kobayashi *Sol State Comm* **83** (1992) 969

41 M S Tyagi *Introduction to Semiconductor Materials and Devices* John Wiley & Sons (1991) 646

42a S K Mandal, D Bhattacharyya, S Chaudhuri and A K Pal *Physics of Semiconductor Nanostructures* (Ed. K P Jain, Narosa) New Delhi (1997) 37

42b S K Kulkarni, A A Khosravi, P Borse, N Deshmukh, W Vogel and J Urban *Physics of Semiconductor Nanostructures* (Ed. K P Jain) Narosa New Delhi (1997) 73

43 N Chestnoy, T D Harris, R Hull and L E Brus *J Phys Chem* **90** (1986) 3393

44 A I Ekimov, I A Kudryavtsev, M G Ivanov and AI L Efros *J Lum* **46** (1990) 83

45 M G Bawendi, P J Corroll, W L Wilson, and L E Brus *J Chem Phys* **96** (1992) 946

46. Y Osaka, K Tsunetomo, F Toyomura, H Myorer and K Kohno *Jap J Appl Phys* **31** (1992) L365

47 K Kohno, Y Osaka, F Toyomura and H Katayama *Jap J Appl Phys* **33** (1994) 6616

48 B Andrianasolo, B Champagnon, M Ferrari and N Neuroth *J Lum* **48-49** (1991) 306

49 M Danek K F Jensen, C B Murray and M G Bawendi *J Cryst Growth* **145** (1994) 714

50 F Hache, M C Klein, D Ricard and C Flytzanis *J Opt Soc America B* **8** (1991) 1802

51 S Farad, R Leon, D Leonard, J L Merz and P M Petroff *Physics Rev B* **52** (1995) 5752

52 AI L Efros, V A Kharchenko and M Rosen *Sol State Comm* **93** (1995) 281